FOUR-WHEEL VEHICLE KINEMATIC AND GEOMETRIC CONSTRAINTS FOR DEFINITION OF TIRE SLIP ANGLE

R. S. VIEIRA*, L. C. NICOLAZZI and N. ROQUEIRO

Department of Mechanical Engineering, Federal University of Santa Catarina, Florianópolis 88040-900, Brazil

ABSTRACT−When considering vehicle safety, tires and all that they represent are a fundamental topic. Tire studies have received a considerable amount of attention from the research community because their improvement has a direct and strong impact on vehicle handling and braking. Within this eld of analysis lies an important behavioral feature: the tire slip angle, which is a consequence of lateral forces acting on the tire. This characteristic is predicted in some cases and evaluated experimentally in others. This paper addresses another way to assess the slip angle. We propose a mathematical model that describes a constraint linking the slip angle and steering angle that make a vehicle turn. We present a simplied kinematic model (based on the classic bicycle model) and a four-wheel model, which makes all of the angles involved compatible with each other. In our case, the match will be given by the determination of the turning radius. Two different scenarios, understeering and oversteering vehicles, were simulated, and the results and conclusions reached are presented herein.

KEY WORDS : Slip angle, Lateral tire model, Vehicle dynamics

1. INTRODUCTION

Vehicle handling is the key consideration in modern vehicle design. Handling is directly associated with safety, and customers constantly seek faster and safer forms of transport. In this regard, tires have played an important role in recent years because their effects are very easy to verify, especially in terms of increasing vehicle safety. In fact, the tires are the only means through which the vehicle interacts with the environment while it is running.

Modern tire studies began in the 1950s (Fiala, 1954) when a mathematical model was proposed to represent the forces acting on a tire and the deformation effects. Several features have an important impact on tire behavior, including the internal pressure, internal and external temperatures, chemical composition of the elastomer, tread pattern and vertical and lateral loads. There are also some implications related to speed, temperature, friction and hysteresis.

Some recent studies have added a significant degree of complexity to tire models, such as the FTire (Flexible Ring Tire model), which was derived from two other tire models presented by the same author, the DNS-Tire model and BRIT (Gipser, 2007). A seminar paper was published in 1998 (Gipser, 1998) at the request of a Japanese OEM. FTire was based on the CTire model, on which research began in 1996 at the request of Germany tire manufacturers (Gipser, 2007). The main difference between the CTire and

FTire models is that the former used the Magic Formula sub-model to model the region outside of the center wheel plane forces and moments. FTire added some degrees of freedom of the original model such that elements are allowed to elongate in the lateral direction. The FTire model has received many improvements to enable the modeling of the self-alignment torque, lateral force, thermo-dynamic issues and tribological structure. Briefly, FTire creates a link between the multi-body and finite-element analyses (DNS-Tire) (Gipser, 2007). The FTire model is a more complex model and has been used in dynamic simulations, which significantly impact the computational and calculation times (Van Oosten, 2007).

However, there are empirical or semi-empirical models that are applicable in several dynamic vehicle studies with relevant impacts in the vehicle industry, such as the Magic Formula of Pacejka (Pacejka and Bakker, 1993). This model was introduced in 1987 (Bakker *et al.*, 1987) and has undergone several improvements in recent years, such as the inclusion of horizontal forces and the pneumatic trail (Pacejka and Bakker, 1993; Kuiper and Van Oosten, 2007). In this model, Pacejka attempts to define a curve that relates the tire slip angle to lateral or longitudinal forces according to the application. Pacejka determines certain values that are useful in constructing curves to determine the slip angle.

Tire studies have received substantial resources; thus, some acronyms have become very familiar to the vehicular research community, such as ACC, ABS, TCS and ESP (Abe, 2009; Hsu *et al.*, 2010). Currently, vehicles have

Corresponding author. e-mail: rvieira@grante.ufsc.br

several electronic components that are responsible for feeling, sensing, reasoning and acting. Adaptive Cruise Control (ACC) plays an important role in considering information on the road conditions from the friction coefficient estimate such that it can adjust the longitudinal spacing headway from the preceding vehicle (Rajamani, 2005). The latest generation of Anti-Lock Brake Systems (ABS) plays an important role in the breaking action, avoiding loss of control and stopping the car to avoid possible obstacles (Ozdalyan, 2008). Traction Control Systems (TCS) must be able to predict the correct tire/road friction coefficient to avoid vehicle slipping and skidding (Canudas de Wit and Tsiotras, 1999; Deur *et al.*, 2001). Similarly, the Electronic Stability Program (ESP) has the ability to create certain forces acting on the tire/ground contact and thus places the vehicle in a stable situation to avoid accidents. To achieve this function, the ESP has to evaluate the value of the tire/road friction coefficient to estimate the vehicle's target yaw rate value (Rajamani, 2005). In all of these systems, it is absolutely necessary to understand the tire/ground properties under dynamic and sometimes chaotic situations, such as a high-speed spin, as well as under stable and static conditions.

Tire studies are commonly divided into two aspects: longitudinal and lateral behavior (Pacejka and Bakker, 1993; Pacejka, 2006; Jazar, 2008). Information regarding the lateral behavior of a tire helps determine the vehicle handling and lateral stability properties (Koo *et al.*, 2006). This field has been extensively explored in control system research, which addresses very accurate tire models to achieve good responses to the dynamic situations that they confront. Lateral forces are responsible for vehicle skid and roll over, and improvements in the lateral tire models have a significant impact on increased vehicle security.

Lateral tire behavior will be the focus area of this study. We will define a mathematical approach for determining the necessary constraints for the slip angles that make the vehicle turn.

The slip angle plays an important role with regards to making the vehicle turn. Some research has been performed in this area, and there are many interesting ways to determine its value. Herein, we are interested in a different point of view because we are looking for a constraint guaranteeing that the vehicle makes an actual turn. Through our model, we will attempt to perform geometric and kinematic analyses, which can represent a rigid relation among all of the vehicle wheels. Linking all of the geometric and kinematic variables of the problem to determine the vehicle cornering trajectory is the central idea of the proposed model. As a result, we can also verify and predict the vehicle behavior by analyzing the lateral acceleration of the rear and front axles. We judge that this can be an important feature of the model as an ESP application.

It is important to note that we will not attempt to estimate the slip angle in this paper; instead, it will be considered an input of our system, similar to a variable that can be read by the sensors. Thus, we can adopt any slip angle estimate to provide the desired value. Some research has been conducted in this context, and there are many interesting ways to determine the slip angle. These methods are based on GPS signals and inertial sensors (Daily and Bevly, 2004; David *et al.*, 2006; Nguyen *et al.*, 2009; Piyabongkarn *et al.*, 2006; Ryan *et al.*, 2009). An innovative steering torque analysis can also be conducted (Hsu *et al.*, 2010), and some publications use ordinary inertial and gyroscope sensors (Farrelly and Wellstead, 1996; Saraf and Tomizuka, 1997; Tseng *et al.*, 1999; Wang *et al.*, 2010).

In section 2, we introduce our proposed model approaching a simple bicycle mode from two different viewpoints, as mentioned above, and the geometric and kinematic models are presented. In section 3, we extend our bicycle model to a complete four-wheel model. Section 4 shows the simulation using the four-wheel model under the oversteering and understeering behavior scenarios. Finally, the results are discussed in section 5.

2. PROBLEM DEFINITION FOR BICYCLE MODEL

In this section, we show the kernel of our model. To simplify the mathematical definition, we will use a bicycle model, which neglects the rolling and camber angle variations. Our approach is based on the geometric and kinematic models. The development of the set of equations is shown in the following subsections.

2.1. Geometric Model

We start our approach from a classical bicycle model without rolling to reduce our problem to three degrees of freedom: the steering angle (δ) and the front (α_f) and rear slip angles (α_r), as shown in Figure 1.

Figure 1 also shows some important vehicle characteristics, including the cornering center (*CC*), the
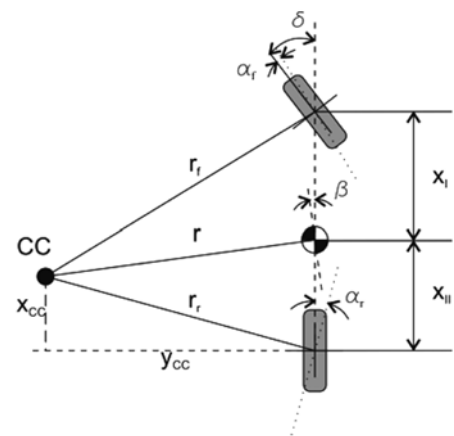

Figure 1. Bicycle model and tire slip angles.

distance between the center of mass and the front axle of the vehicle (X_I), the distance between the center of mass and the rear axle of the vehicle (X_{II}), the vehicle slip angle (β), as proposed by (Rajamani, 2005), the distance between the center of the rear wheel and the cornering center in the longitudinal direction of the vehicle (x_{CC}), the distance between the center of the rear wheel and the cornering center in the transversal direction of the vehicle (y_{CC}), the turning radius of the vehicle center of mass (r), the turning radius of the front axle center (r_f), and the turning radius of the rear axle center (r_r). In this article, we will use the X, Y and Z axles, which are the longitudinal, lateral, vertical vehicle axles, respectively, as the coordinate system. The vertical axles have the negative direction to the ground.

We can deduce that some constraints can be imposed in our model based on geometric relations. Thus, we can determine the cornering center coordinates from the rear axle center. Trigonometrically,

$$x_{CC} = r_r \sin \alpha_r \tag{1}$$

and

$$y_{CC} = \sqrt{r^2 - (X_{II} - x_{CC})^2} \tag{2}$$

Substituting the x_{CC} value given by Equation (1) in Equation (2), we can deduce the coordinates using the rear slip angle, turning radius and vehicle wheelbase (L).

$$y_{CC} = \sqrt{r^2 - ((1-a)L - r_r \sin \alpha_2)^2} \tag{3}$$

where $a = X_I/L$.

In the same manner, the front turning radius is shown below.

$$r_f = \sqrt{(X_I + X_{II} - X_{CC})^2 + y_{CC}^2} \tag{4}$$

Substituting the x_{CC} and y_{CC} values given by Equations (1) and (3) and the X_I and X_{II} values given by the vehicle wheelbase relation, the first equation relating the front radius (r_f), rear radius (r_r) and center-of-mass radius (r) is as follows:

$$r_f = \sqrt{r^2 + 2aL^2 - a^2L^2 - 2aLr_r \sin \alpha_r} \tag{5}$$

According to Figure 1, we can assume another relation between the front (r_f) and rear radius (r_r), as shown below:

$$r_f \cos(\delta - \alpha_f) = r_r \cos \alpha_r \tag{6}$$

Solving equations (5) and (6), we have by approximation:

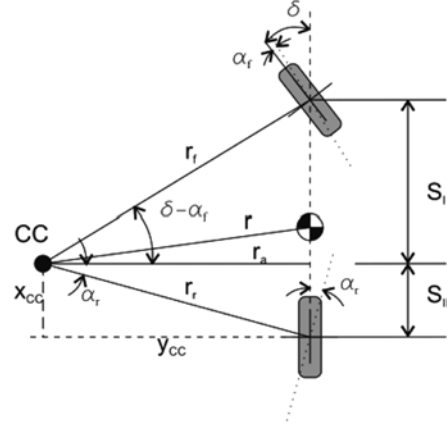$$r_f = \sqrt{C_1 - 2aL \sin \alpha_r \sqrt{C_2}} \tag{7}$$

Figure 2. Linking steering angle and slip angles.

$$r_r = \sqrt{C_2} - \frac{aL \cos^2(\delta - \alpha_f) \tan \alpha_r}{\cos \alpha_r} \tag{8}$$

where

$$C_1 = 2aL^2 - a^2L^2 + r^2 + 2a^2L^2 \cos^2(\delta - \alpha_f) \tan^2 \alpha_r \tag{9}$$

$$C_2 = \left(\frac{\cos(\delta - \alpha_f)}{\cos \alpha_r}\right)(2aL^2 - a^2L^2 + r^2 + a^2L^2 \cos^2(\delta - \alpha_f) \tan^2 \alpha_r) \tag{10}$$

Another geometrical assumption is based on the cornering center. According to Figure 2, we can propose two new values, S_I and S_{II}, which define the distances between the orthogonal projection of the cornering center in the longitudinal direction and both axles.

$$S_I = r_a \tan(\delta - \alpha_f) \tag{11}$$

$$S_{II} = r_a \tan \alpha_r \tag{12}$$

where r_a is the actual turning radius, which differs from the center-of-mass radius and each wheel turning radius. It is important to understand that the actual radius (r_a) will only be the same as the rear radius (r_r) in the absence of the tire slip angle. In this case, the cornering center (CC) will be placed over the rear axle line, and x_{CC} will be null.

From the geometrical model (Figure 2), we can conclude that:

$$L = S_I + S_{II} \tag{13}$$

Substituting the S_I and S_{II} values of equations (11) and (12) in equation (13), we arrive at:

$$r_a = \frac{L}{\tan(\delta - \alpha_f) + \tan \alpha_r} \tag{14}$$

Finally, we can relate the actual turning radius to the center-of-mass turning radius through the model shown in
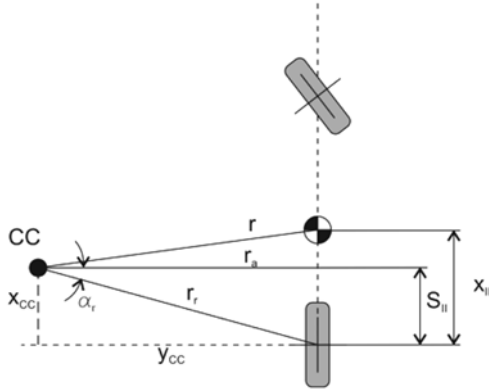
Figure 3. Definition of the center-of-mass turning radius.

Figure 3.

$$r = \sqrt{r_a^2 + (X_{II} - S_{II})^2} \tag{15}$$

2.2. Kinematic Model

To include some other constraints in our model, we will start from the assumption that each vehicle component must have the same angular velocity ($\dot{\psi}$) such that:

$$\dot{\psi} = \frac{V}{r} = \frac{V_f}{r_f} = \frac{V_r}{r_r} \tag{16}$$

In other words, the translational velocities can be given by:

$$V = \dot{\psi}r \qquad V_f = \dot{\psi}r_f \qquad V_r = \dot{\psi}r_r \tag{17}$$

It is interesting to note that the approach proposed by (Rajamani, 2005) admits small slip angles and that the wheelbase is small compared to the turning radius r. Thus, $V/r = \delta/L$ is impossible here because the slip angles are considered.

We can also define the velocity components of each wheel as:

$$u_f = \dot{\psi}r_f \cos(\delta - \alpha_f) \qquad u_r = \dot{\psi}r_r \cos\alpha_r \tag{18}$$

$$v_f = \dot{\psi}r_f \sin(\delta - \alpha_f) \qquad v_r = \dot{\psi}r_r \sin\alpha_r \tag{19}$$

where u_f and v_f are the X- and Y-direction velocities of the front wheel, respectively, and u_r and v_r are the respective velocities for the rear wheel.

With this set of equations, we can determine the kinematics of our model, stabling a constrained relation among all of the angles acting on the cornering center. The next section describes the improvement of our model to a four-wheel model.

3. FOUR-WHEEL MODEL

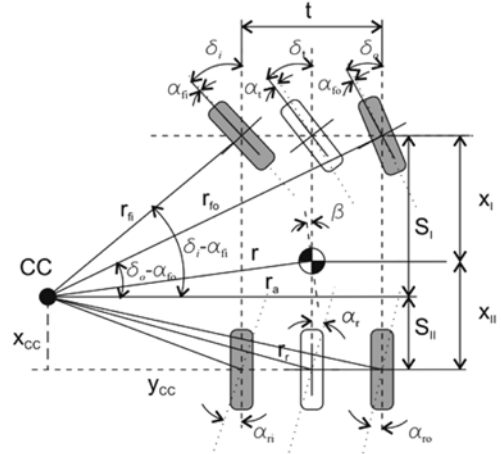We will analyze a four-wheel vehicle problem in a similar

Figure 4. Combination of the bicycle and four-wheel vehicle models.

manner as the bicycle model. The geometric and kinematic models will be presented and then matched at the end of this section.

3.1. Geometric Model

The starting point of our four-wheel vehicle model will be the bicycle model described above. Figure 4 presents the two models together, linking all of the slip angles to the same cornering center. The bicycle model will form the basis of the four-wheel model solution.

We can analyze this model using the defined values of α_r and α_f; however, they are no longer input values of the problem. In this case, they are theoretical values, and they cannot be read by all types of measurement systems. In fact, they do not physically exist. However, we have the following four new different slip angles:

- α_{fi} - Front slip angle of the inside cornering wheel;
- α_{fo} - Front slip angle of the outside cornering wheel;
- α_{ri} - Rear slip angle of the inside cornering wheel;
- α_{ro} - Rear slip angle of the outside cornering wheel.

In our approach, we will considerer two inputs: the inside cornering wheel slip angles, α_{fi} and α_{ri}. The respective outside angles are related to these inputs by
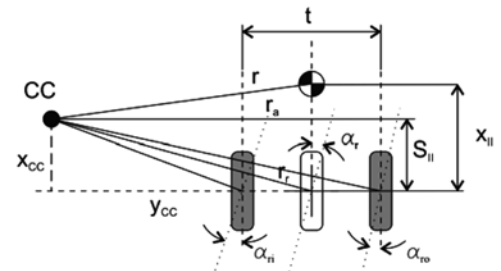

Figure 5. Rear axle geometrical entities.

geometric constraints, as discussed below.

We start our model from the rear axle, as shown in Figure 5. We can relate the geometrical entities of the rear axle, such as the angles and radii, to one another.

From Figure 2, we have:

$$\alpha_r = \arctan\left(\frac{S_{II}}{r_\alpha}\right) \tag{20}$$

In a similar manner, we can determine the following from Figure 5:

$$\alpha_{ri} = \arctan\left(\frac{S_{II}}{r_\alpha - t/2}\right) \qquad \alpha_{ro} = \arctan\left(\frac{S_{II}}{r_\alpha + t/2}\right) \tag{21}$$

We can rearrange equations 21 to give:

$$S_{II} = (r_\alpha - t/2)\tan\alpha_{ri} \qquad S_{II} = (r_\alpha + t/2)\tan\alpha_{ro} \tag{22}$$

Then, from setting both equations equal to one another, we find the relation between α_{ri} and α_{ro} shown below.

$$\frac{\tan\alpha_{ri}}{\tan\alpha_{ro}} = \frac{r_\alpha + t/2}{r_\alpha - t/2} \tag{23}$$

By isolating the actual radius from equation (23), we have:

$$r_\alpha = \frac{t}{2}\frac{\tan\alpha_{ri}}{\tan\alpha_{ri} - \tan\alpha_r} \tag{24}$$

We can use the same approach for the vehicle front axle, as shown in Figure 6.

We can also relate the vehicle geometry to the slip angles, as described above. In this case, we also have the presence of the steering angle:

$$\delta_{fi} - \alpha_{fi} = \arctan\left(\frac{S_I}{r_a - t/2}\right) \qquad \delta_{fo} - \alpha_{fo} = \arctan\left(\frac{S_I}{r_a + t/2}\right) \tag{25}$$

From the bicycle model, we can determine that:

$$S_I = r_a\tan(\delta_f - \alpha_f) \tag{26}$$

$$S_{II} = r_a\tan\alpha_r \tag{27}$$

From equation (26), we can conclude that the value ($\delta_f - \alpha_f$) can be considered the desired steering angle such that S_I

Figure 6. Front axle geometrical entities.

tends toward L and r_a tends towards r_r. This tendency produces a desirable steering angle that can be considered the required steering angle for a given turning radius. This angle will be denoted by δ_d and is an input of the vehicle driver that can be used to determine a desirable solution from the geometrical viewpoint.

We also know that:

$$S_{II} = L - S_I \tag{28}$$

and by substituting the S_I value given by equation (26) in equation (28), we obtain:

$$S_{II} = L - r_a\tan\delta_d \tag{29}$$

By setting equations (27) and (29) equal to one another, we have:

$$r_a = \frac{L}{\tan\alpha_r - \tan\delta_d} \tag{30}$$

With this radius value, we can evaluate S_I and include the following additional geometrical constraints:

$$\tan(\delta_i - \alpha_{fi}) = \frac{S_{Ii}}{r_a - t/2} \qquad \tan\delta_d = \frac{S_I}{r_a} \tag{31}$$

By isolating S_I in equations (31), we can establish the following relation with the actual radius:

$$r_a = \frac{t}{2}\frac{\tan(\delta_i - \alpha_{fi})}{\tan(\delta_i - \alpha_{fi}) - \tan\delta_d} \tag{32}$$

By setting equations (24) and (32) equal to one another, the following relation between the desired steering angle (δ_d) and inner wheel slip angles (α_{fi} and α_{ri}) is found:

$$\frac{\tan\alpha_{ri}}{\tan\alpha_{ri} - \tan\alpha_r} = \frac{\tan(\delta_i - \alpha_{fi})}{\tan(\delta_i - \alpha_{fi}) - \tan\delta_d} \tag{33}$$

By subtracting equations (31) from this term, we have:

$$\frac{t}{2S_I} = \frac{1}{\tan(\delta_i - \alpha_{fi})} - \frac{1}{\tan\delta_d} \tag{34}$$

In the same manner, we can relate the outside steering angle through:

$$\frac{t}{2S_I} = \frac{1}{\tan(\delta_o - \alpha_{fo})} - \frac{1}{\tan\delta_d} \tag{35}$$

By setting equations (34) and (35) equal to one another, we obtain

$$\frac{\tan(\delta_o - \alpha_{fo})}{\tan(\delta_i - \alpha_{fi})} = 1 \tag{36}$$

Thus, regardless of the values for the slip angles and steering angles, the difference between them for each front wheel will always be the same. Thus, we can dene each steering angle with the assumption of the absence of a slip angle. The steering angle will only be a function of the steering system, as shown below.
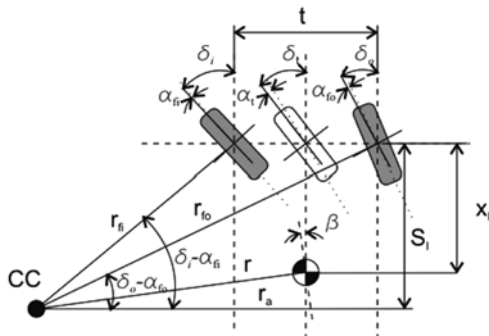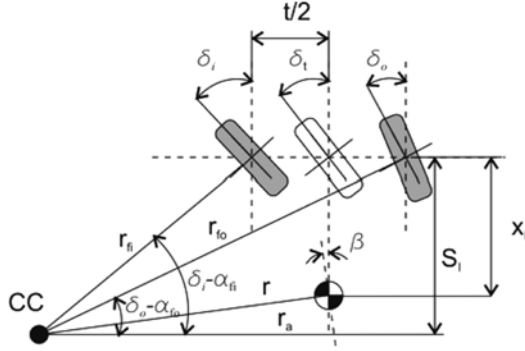
Figure 7. Relation between the inner and desired steering angles.

$$\frac{t}{L} = \frac{1}{\tan \delta_o} - \frac{1}{\tan \delta_i} \tag{37}$$

We can also relate the inside to the desired steering angles considering only half of the car, as shown in Figure 7.

In this case, we can dene the inner steering angle as

$$\delta_i = \arctan\left[\frac{2L}{2L\cot\delta_d - t}\right] \tag{38}$$

Using equation (24), this definition helps us dene the actual turning radius (r_a), which in turn can be used to nd S_{II} (equation (29)) and S_I (equation (28)).

With the value given by equation (24), we can evaluate the center-of-mass radius, which is defined as:

$$r = \sqrt{r_a^2 + (X_{II} - S_{II})^2} \tag{39}$$

where S_{II} is given by equation (27).

Having obtained the actual radius (r_a), desired steering angle (δ_d), inside and outside front slip angles (α_{fi} and α_{fo}), and inside and outside steering angles (δ_i and δ_o), we can dene all of the radii as

$$r_{fi} = \sqrt{(r_a - t/2)^2 + S_I^2} \tag{40}$$

$$r_{fo} = \sqrt{(r_a + t/2)^2 + S_I^2} \tag{41}$$

$$r = \sqrt{r_a^2 + (X_{II} - S_{II})^2} \tag{42}$$

$$r_{ri} = \sqrt{(r_a - t/2)^2 + S_{II}^2} \tag{43}$$

$$r_{ro} = \sqrt{(r_a + t/2)^2 + S_{II}^2} \tag{44}$$

3.2. Kinematic Model

The same assumption applied to the bicycle model is proposed here, that is, "all vehicle parts have the same cornering center, and thus, the angular velocity related to this point is the same".

This helps us determine the following relation:

$$\dot\psi = \frac{V}{r} = \frac{V_f}{r_f} = \frac{V_r}{r_r} = \frac{V_{fi}}{r_{fi}} = \frac{V_{fo}}{r_{fo}} = \frac{V_{ri}}{r_{ri}} = \frac{V_{ro}}{r_{ro}} \tag{45}$$

where V_{fi} is the translational speed of the inside wheel of the front axle, V_{fo} is the translational speed of the outside wheel of the front axle, V_{ri} is the translational speed of the inside wheel of the rear axle and V_{ro} is the translational speed of the outside wheel of the rear axle.

We can also admit that each axle is sufficiently rigid to transmit the same speed components in the X- and Y-directions. This can be modeled by the following equations for the rear axle:

$$u_{ri} = u_r = u_{ro} \qquad v_{ri} = v_r = v_{ro} \tag{46}$$

$$\begin{aligned} V_{ri}\cos\alpha_{fi} = V_f\cos\alpha_f = V_{fo}\cos\alpha_{fo} \\ V_{fi}\sin\alpha_{fi} = V_f\sin\alpha_f = V_{fo}\sin\alpha_{fo} \end{aligned} \tag{47}$$

and through the following equations for the front axle:

$$u_{fi} = u_f = u_{fo} \qquad v_{fi} = v_f = v_{fo} \tag{48}$$

$$\begin{aligned} V_{fi}\cos\alpha_{fi} = V_f\cos\alpha_f = V_{fo}\cos\alpha_{fo} \\ V_{fi}\sin\alpha_{fi} = V_f\sin\alpha_f = V_{fo}\sin\alpha_{fo} \end{aligned} \tag{49}$$

With this set of equations, we can determine the kinematics of our model and establish a constrained relation between all of the angles acting during the cornering. We can combine all of these to determine the constraints leading to the following scenario: three inputs, δ_d, α_{ri}, and α_{fi}. With these values, we can use modied equation (37), which relates the desired steering angle and the inside cornering steering angle as shown below:

$$\frac{1}{\tan \delta_d} - \frac{1}{\tan \delta_i} = \frac{t}{2L} \tag{50}$$

We can also dene the rear axle slip angle (α_r), which is given by equation (33). It is important to note that we desire an input of δ_d to steering that produces δ_i in the inner wheel, but the actual radius will be determined by including the effect of the slip angle as follows:

$$r_a = \frac{\delta_I}{\tan(\delta_i - \alpha_{fi})} + \frac{t}{2} = \frac{\delta_I}{\tan \delta_d} \tag{51}$$

By rearranging equation (51), we have

$$S_I = \frac{t}{2\left[\dfrac{1}{\tan \delta_d} - \dfrac{1}{\tan(\delta_i - \alpha_{fi})}\right]} \tag{52}$$

We can then dene the actual radius through equation (51) and all of the other values defined by equations (40) to (44). The next step was to simulate our model in a numeric tool. Some interesting results were obtained from this simulation, as described in the next section.

4. SIMULATING THE MODEL

In this section, we show the simulation of the four-wheel model. We created a Simulink block to be incorporated into the Matlab software. First, we present the main features of
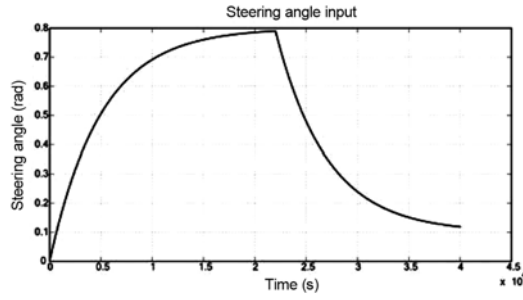
Figure 8. Steering angle input data.

the simulation process, followed by some graphs.

4.1. Describing the Input Signals

Our four-wheel model uses the following five inputs to characterize the vehicle:

- Vehicle wheel base (L) in meters;
- Vehicle track (t) in meters;
- Desirable steering angle (δ_d);
- Front inner wheel slip angle (α_{fi}); and
- Rear inner wheel slip angle (α_{ri}).

The desirable steering angle can be considered an angular encoding attached to the steering wheel that takes the reduction ratio into account. In our simulation, we adopted the cornering prole shown in Figure 8.

In this action, we have a smooth cornering to the right, a small period with a stable steering angle and a fast return to the center position of the steering wheel.

We introduce two approaches, simulation 01 and simulation 02. In the rst approach, we considered that the front slip angle is approximately three times greater than the rear slip angle, as shown in Figure 9.

The second simulation has an inverted situation, where the rear slip angle is greater than the front slip angle, as shown in Figure 10. In both situations, a variation in the slip angle as a function of the inertial force caused by the variation in the turning radius was imposed. The values lie within a reasonable range and thus could be used for the model testing.
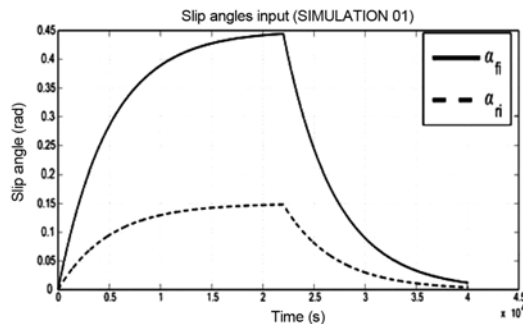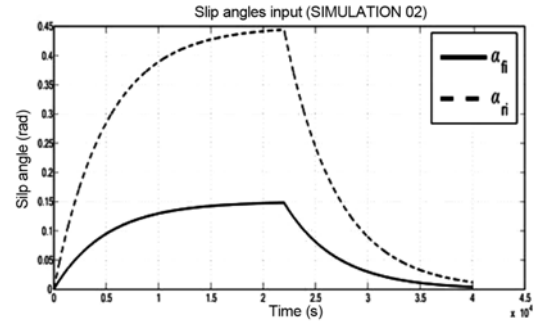

Figure 9. Slip angle inputs for simulation 01.

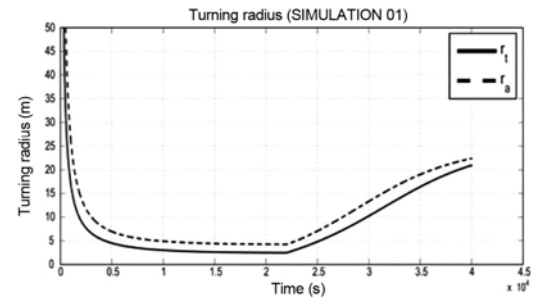Figure 10. Slip angle inputs for simulation 02.

Figure 11. Turning radius for simulation 01.

We also considered the following aspects of the car: 2.5 m of wheelbase, 64% of the weight over the front axle, and 1.4 m of track. In our simulation, the vehicle has the same track for the front and rear axles.

4.2. Analyzing the Results for Simulation 01

The starting point of our analysis was the turning radius, which is shown in Figure 11 for the rst simulation.

To analyze the results, we introduced a new concept called the theoretical radius (r_t), which is represented by the solid line in Figure 11. This radius can be evaluated as

$$r_i = \frac{L}{\tan \delta} \tag{53}$$

It is a theoretical value representing the turning radius without slip and can be used to understand the dynamic behavior of the vehicle. In simulation 01 (front slip angle greater than the rear slip angle), the theoretical radius is always smaller than the actual radius (see Figure 11), indicating that the vehicle is cornering a turn that is bigger than the theoretical corner. Thus, to turn the right corner, the driver must steer more. In other words, in this type of vehicle, the drive must steer more than the actual cornering track. The front axle tends to move outside of the cornering center, indicating understeering behavior.

Our model also supplies the lateral speed, as shown in Figure 12.

The rear axle has a maximum positive value of 2.5 m/s for a vehicle running speed of 20 m/s. At the same point,
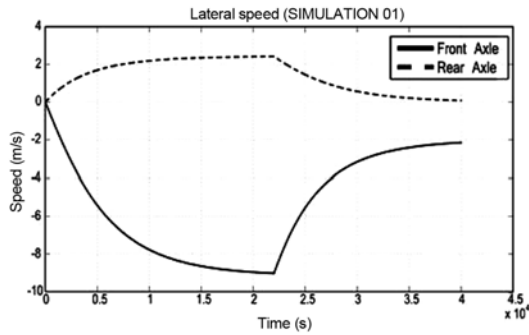
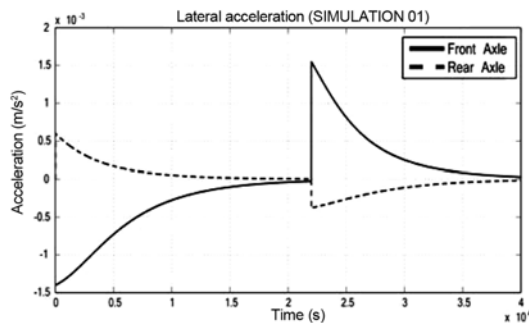Figure 12. Lateral speed of the front and rear outer wheels for simulation 01.

Figure 13. Lateral acceleration of the front and rear outer wheels for simulation 01.

Figure 15. Lateral speed of the front and rear outer wheels for simulation 02.
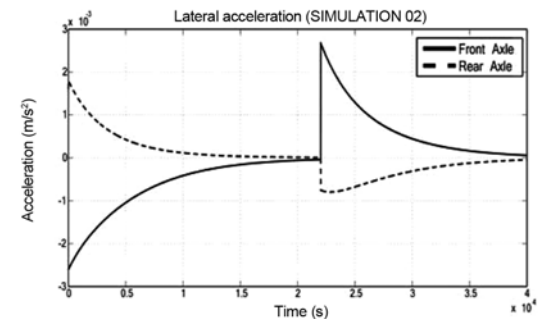
Figure 16. Lateral acceleration of the front and rear outer wheels for simulation 02.

the front axle has a maximum value of approximately 9 m/s in the opposite direction (inside cornering) and changes gradually, following the change in the steering angle (Figure 8).

In this simulation, we found a maximum yaw rate of 4.57 rad/s, maintaining the translational speed of 20 m/s and the lateral acceleration of each axle, as shown in Figure 13.

4.3. Analyzing the Results for Simulation 02

In this case, we changed the slip angles to be greater in the rear axle. Following the same methodology used in simulation 01, we obtained the turning radius results shown
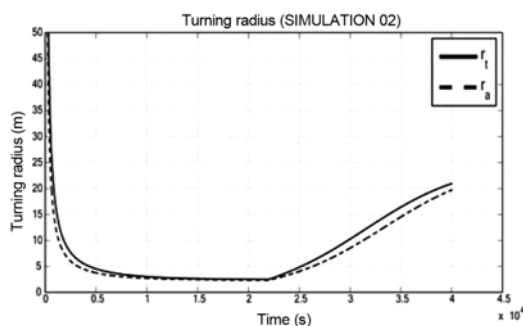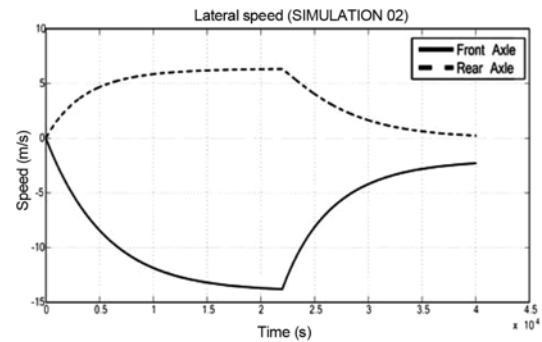

Figure 14. Turning radius for simulation 02.

in Figure 14.

These values differ from those obtained in the rst simulation. The theoretical radius is now larger than the actual radius, indicating that the vehicle tends to trace a corner smaller than the real corner. In this case, the driver must decrease the steering angle to correct the cornering path. This action is typically referred to as counter-steering, which indicates that the vehicle is oversteering.

The same procedure was applied to the lateral speed, as shown in Figure 15.

By comparing these values to those in Figure 12, we can observe that for the same running speed of 20 m/s, we have higher values of approximately 6 m/s for the rear axle and 14 m/s for the front axle in the opposite direction. These results are consistent with the consolidated knowledge that oversteering vehicles are fast at cornering paths. This conclusion is reinforced by the maximum yaw rate value of 8.04 rad/s, which is almost twice that of the rst simulation.

To conclude our analysis, the lateral acceleration is shown in Figure 16.

5. CONCLUSIONS AND FUTURE WORK

Tires now represent an important research topic worldwide, and the impact of the results acquired makes vehicles safer every day. In this context, we have presented a new

approach for the tire slip angle, which is another important safety factor. We presented a simple model based on a bicycle model, which was the starting point of this new way to approach the slip angle. We believe that the model presented in this paper could provide the analytical solution for constraining the handling of vehicle dynamics.

We noted that the results reported herein are consistent with the knowledge available on oversteering and understeering vehicles. Our model represented the expected results regarding vehicle behavior and slip angles. When applying this approach, we constrained three inputs so the vehicle could corner in a reasonable radius. In fact, this model does not consider driver control, and its results correspond to a non-reactive action. The results show that the cornering center is continuously changing because it is a function of the slip angles, which are variables in our input data. An important improvement to this model could be designing a driver model that reacts, applying counter-steering when needed.

Using this model, we also verified that oversteering vehicles generate more lateral acceleration than those that understeer. However, we neglect some features in this model. For instance, we do not consider that the tire can transfer the entire lateral load linked to the acceleration values. In kinematics, we are not concerned with forces; thus, the friction coefficient of the tire/ground interface is not relevant at this point.

Our model produced coherent values, as the outer cornering slip angles could be determined from the inner cornering slip angles. Thus, the vehicle can turn like a rigid object. We also found that the speeds are consistent with the radius, and the geometric and kinematic constraints proposed here can thus be used to develop a complete kinematic model. The accelerations produced by our model will also be useful for the future development of a dynamic model development. This can be helpful for an ESP program. The lateral acceleration values can easily represent the vehicle tendency to oversteer or understeer, and as a result, the ESP can act faster by an active manner. These values can predict when the driver will lose control.

We reached the proposed objective to represent a mathematical model that generates the cornering center from the steering and slip angles. The numerical model also provides acceleration values that can be used in dynamic models. In this regard, this model can be used to determine lateral loads and maximum supported values.

This study forms part of our research on small narrow vehicles (Vieira et al., 2007; Roqueiro and Colet, 2010; Roqueiro et al., 2010), and in this context, we plan to use these results in models currently being developed. To reach that aim, our next steps are to improve this model to a three-wheel model and adapt the new model to a vehicle that we are currently working on. The new three-wheel model will include some features that are not shown here, such as the rolling angle and wheel camber variation.

REFERENCES

Abe, M. (2009). Vehicle Handling Dynamics. Butterworth-Heinemann. Elsevier. Oxford. UK.

Bakker, E., Nyborg, L. and Pacejka, H. B. (1987). Tyre modelling for use in vehicle dynamics studies. *Society of Automotive Engineers Int. Cong. and Expo,* Detroit, MI.

Canudas de Wit, C. and Tsiotras, P. (1999). Dynamic tire friction models for vehicle traction control. *Proc. 38th IEEE Conf. Decision and Control*, Phoenix, AR, 3746–3751.

Daily, R. and Bevly, D. M. (2004). The use of GPS for vehicle stability control systems: Industrial electronics. *IEEE Trans. Industrial Electronics* **51**, 2, 270–277.

David, M. B., Ryu, J. and Gerdes, J. C. (2006). Integrating INS sensors with GPS measurements for continuous estimation of vehicle side slip, roll, and tire cornering stiffness. *IEEE Trans. Intelligent Transportation Systems*, **7**, 483–493.

Deur, J., Asgari, J. and Hrovar, D. (2001). A dynamic tire friction model for combined longitudinal and lateral motion. *ASME-IMECE World Conf.*, **2**, New York, 1–8.

Farrelly, J. and Wellstead, P. (1996). Estimation of vehicle lateral velocity. 1996 *IEEE Int. Conf. Control Applications*. Dearborn, MI, 552–557.

Fiala, E. (1954). Seitenkrafte am rollenden luftreifen. VDI *Zeitschrift*, **96**, Germany.

Gipser, M. (2007). FTire : The tire simulation model for all applications related to vehicle dynamics. *Vehicle System Dynamics: Int. J. Vehicle Mechanics and Mobility*, **45** (1 supp 1), 139–151.

Gipser, M. (1998). *Reifenmodelle für Komfort- und Schlechtwegsimulationen.* Aachener Kolloquium Fahrzeug-und Motorentechnik. Aachen. Germany.

Hsu, Y.-H. J., Laws, S. M. and Gerdes, J. C. (2010). Estimation of tire slip angle and friction limits using steering torque. *IEEE Trans. Control Systems Technology*, **18**, 896–907.

Jazar, R. N. (2008). *Vehicle Dynamics: Theory and Application*. Springer. Germany.

Koo, S. L., Tan, H. S. and Tomizuka, M. (2006). An improved tire model for vehicle lateral dynamics and control. *2006 American Control Conf.*, Minneapolis, MI, 5879–5884.

Kuiper, E. and van Oosten, J. J. M. (2007). The PAC2002 advanced handling tire model. *Vehicle System Dynamics*, **45**, 153–167.

Nguyen, H., Kang, H.-J., Suh, Y.-S. and Ro, Y.-S. (2009). INS/GPS integration system with DCM based orientation measurement. *Emerging Intelligent Computing Technology and Applications*, **5754**, 856–869.

Ozdalyan, B. (2008). Development of slip control anti-lock braking system model. *Int. J. Automotive Technology* **9**, 1, 71–80.

Pacejka, H. B. (2006). *Tire and Vehicle Dynamics*. 2nd Edn. SAE. USA.

Pacejka, H. B. and Bakker, E. (1993). The magic formula tyre model. *Vehicle System Dynamics*, **21**, 1–18.

Piyabongkarn, D., Rajamani, R., Grogg, J. A. and Lew, J. Y. (2009). Development and experimental evaluation of a slip angle estimator for vehicle stability control: Control systems technology. *IEEE Trans. Control Systems Technology* **17**, **1**, 78–88. 1063–6536.

Rajamani, R. (2005). *Vehicle Dynamics and Control.* Springer.

Roqueiro, N. and Colet, E. F. (2010). A sliding mode controlled three wheels narrow vehicle for two passengers. *11th Int. Workshop on Variable Structure Systems (VSS)*, Mexico, 358–363.

Roqueiro, N., Vieira, R. S. and Faria, M. G. (2010). Tilting control of a three-wheeled vehicle by steering. *CBA 2010 - XVIII Cong. Brasileiro de Automatica*, Bonito, Brazil, 3464–3471.

Ryan, J., Bevly, D. and Lu, J. (2009). Robust sideslip estimation using GPS road grade sensing to replace a pitch rate sensor. *IEEE Int. Conf. Systems, Man and Cybernetics (SMC'09)*, Piscataway, NJ, 2026–2031.

Saraf, S. and Tomizuka, M. (1997). Slip angle estimation for vehicles on automated highways. *Proc. 1997 American Control Conf.*, **3**, 1588–1592.

Tseng, H. E., Madau, D., Ashrafi, B., Brown, T. and Recker, D. (1999). Technical challenges in the development of vehicle stability. *Proc. 1999 IEEE Int. Conf. Control Applications*, **2**, 1660–1666.

Van Oosten, J. J. M. (2007). TMPT tire modeling in ADAMS. *Vehicle System Dynamics: Int. J. Vehicle Mechanics and Mobility*, **45**, 191–198.

Vieira, R. S., Nicolazzi, L. C., Roqueiro, N. and Padilha, R. (2007). Modeling and analysis of dynamic behavior of tilting vehicle. *XVI Cong. e exposição Internacionais da Tecnologia da Mobilidade*. Sao Paulo. Brazil.

Wang, W., Yuan, L., Tao, S., Zhang, W. and Su, T. (2010). Estimation of vehicle side slip angle in nonlinear condition based on the state feedback observer. *IEEE Int. Conf. Automation and Logistics (ICAL)*. Hong Kong, Macau, 632–636.